

SLAC – PUB – 3714
June 1985
(T)

Discretized Light-Cone Quantization: Solution to a Field Theory in One-Space-One-Time Dimensions.*

HANS-CHRISTIAN PAULI[†]

and

STANLEY J. BRODSKY

*Stanford Linear Accelerator Center
Stanford University, Stanford, California, 94305*

ABSTRACT

In an earlier paper, the field theoretic bound state problem in 1+1 dimension was mapped to the problem of diagonalizing a strictly finite dimensional Hamiltonian matrix by quantizing at equal light cone time. In this paper, we calculate the invariant mass spectrum for the Yukawa theory $\bar{\psi}\varphi\psi$. The spectrum is shown to be independent of the momentum cut-off in the limit $\Lambda \rightarrow \infty$ and more complex with increasing harmonic resolution K . The results are compared with the recent work of Brooks and Frautschi, who apply conventional space-time quantization. Because of incompatible cut-offs, we reproduce their results only qualitatively, for a rather small value of Λ . We propose an explanation for their non-unique mass renormalization. We also discuss the straightforward application of the discretized light-cone quantization to non-Abelian field theories in 1+1 dimension, and the generalization to 3+1 dimensions.

Submitted to *Physical Review D*

* Work supported by the Department of Energy, contract DE – AC03 – 76SF00515.

† On leave from Max-Planck-Institut für Kernphysik, Heidelberg, Germany

1. Introduction

Consider a Fermi field coupled to a Bose field by the trilinear form $\lambda\bar{\psi}\varphi\psi$. In one time and one space dimension, one has 3 constants of motion: the total energy E , the total momentum P , and the total charge Q . Here E and P are components of a Lorentz vector, whose contraction is the invariant mass squared $M^2 = E^2 - P^2$. Upon quantization at equal time, E , P , Q and M^2 become operators which commute mutually. Their simultaneous diagonalization is equivalent to solving the equations of motion for the operator fields, i.e. the Klein-Gordon and the Dirac equations. Brooks and Frautschi^[1] have studied this problem numerically in the “number” or Fock space representation. The number of Fock states with the same P and the same Q has no upper limit, the dimension of the Hamiltonian matrix is therefore unlimited as well. By introducing an artificial length L and a momentum cut-off Λ , the matrix can be made finite, though large, and can be diagonalized numerically. One must then be able to show that physically relevant results do not depend on either L or Λ . Because of the difficulty of the numerical work this has not been done in practice.

The same problem can be treated in a different way^[2] by quantizing the fields at equal light cone time $\tau = t + x$. Again one has 3 constants of motion, but they appear as the total *light cone* energy $P^- = E - P$, the total *light cone* momentum $P^+ = E + P$, and the charge Q . The operators P^- and P^+ are again components of a Lorentz vector, whose contraction is the invariant $M^2 = P^+P^-$. Since Q , P^\pm commute mutually, they can be diagonalized simultaneously. One can formulate the problem in Fock space representation, introducing again two formal parameters, a box size L and an ultraviolet regulator Λ . Thus far everything is analogous, if not identical, to the usual quantization; in fact, if done correctly, one can switch back and forth between space-time and light cone quantization, since the representations are connected by a unitary transformation. But there is an essential difference: on the light cone only a *finite number of Fock states* can have the same (light cone) momentum and the same charge, and therefore

the mass matrix has a finite dimension to begin with. All this was discussed at length in paper I^[2], as well as the fact that the operator $M^2 = P^+P^-$ is strictly independent of the box size L .

The present work has three objectives. (1) We demonstrate, that the physical results, the mass spectra and the eigenstates, become independent of the cut-off Λ in the limit $\frac{1}{\Lambda} \rightarrow 0$. This is discussed in sections 3 and 4. (2) We show that the discretized light-cone quantization method as developed in the earlier paper^[2] is feasible, and that no difficulties arise obtaining numerical solutions for the bound state spectrum and the bound state wavefunctions. In some cases we give exact analytical solutions (see section 3). In the same section, we discuss the question of renormalization. In order not to overload the paper with numerics, we restrict ourselves to the charge 0 and charge 1 sectors. (3) Last but not least, we convince ourselves (in section 5), that the numerical results obtained with light-cone quantization are not in conflict with those of space-time quantization.^[1]

In section 6, we summarize the main results, and discuss discretized light-cone quantization, in particular to which extent the case of scalars in 1+1 dimensions might be useful for developing methods suitable for the more interesting fields in 3+1 dimensions.

2. The Model and the Notation.

The Lagrangian density

$$\mathcal{L} = \frac{1}{2} \partial^\mu \varphi \partial_\mu \varphi + \frac{1}{2} m_B^2 \varphi^2 + \frac{i}{2} \bar{\psi} \gamma^\mu \partial_\mu \psi - \frac{i}{2} \partial_\mu \bar{\psi} \gamma^\mu \psi - (m_F + \lambda \varphi) \bar{\psi} \psi . \quad (2.1)$$

specifies the physics of a fermion field ψ interacting with a boson field φ . In one space and one time dimension, the canonical procedure generates three constants of the motion. In light cone notation^[2], they are the total (light cone) momentum P^+ , the total (light cone) energy P^- , and the total charge Q . If one expands the fields into plane waves, and requires them to be periodic operator functions on the

light cone space interval $(-L, L)$, then Q, P^+ and P^- become operators acting in Fock space, i.e. they can be expressed in terms of creation and destruction operators for fermions (i.e. b_n^\dagger and b_n), antifermions (i.e. d_n^\dagger and d_n), and bosons (i.e. a_n^\dagger and a_n), which obey the usual commutation relations. More specifically, one writes the fields as

$$\begin{aligned}\varphi(x) &= \sum_{n=1}^{\Lambda} \frac{1}{\sqrt{4\pi n}} (a_n e^{-ik_n^+ x_\nu} + a_n^\dagger e^{+ik_n^+ x_\nu}), \quad \text{and} \\ \psi(x) &= \sum_{n=1}^{\Lambda} \frac{u}{\sqrt{2L}} (b_n e^{-ik_n^+ x_\nu} + d_n^\dagger e^{+ik_n^+ x_\nu}),\end{aligned}\tag{2.2}$$

with discretized single particle light cone momenta

$$k_n^+ = \frac{2\pi}{L} n, \quad n = 1, 2, \dots, \Lambda. \tag{2.3}$$

The single particle light cone energies are

$$k_n^- = \frac{m_F^2}{k_n^+} \quad \text{and} \quad k_n^- = \frac{m_B^2}{k_n^+}, \tag{2.4}$$

for fermions and bosons, respectively. The spinor u is independent of n . One should note the introduction of two additional and formal parameters, i.e. the *box size* L , and the maximum single particle momentum, the *cut-off* Λ .

As a peculiarity of working on the light cone, one can isolate all the dependence on the *light-cone box size* L rather neatly, i.e.

$$P^+ = \frac{2\pi}{L} K \quad \text{and} \quad P^- = \frac{L}{2\pi} H, \quad \text{thus} \quad M^2 \equiv P^+ P^- = KH, \tag{2.5}$$

and work with the operators K and H which do not depend on L .

In the Fock space representation, two of the three operators are already diagonal:

$$Q = \sum_n b_n^\dagger b_n - d_n^\dagger d_n \quad \text{and} \quad K = \sum_n n(a_n^\dagger a_n + b_n^\dagger b_n + d_n^\dagger d_n). \quad (2.6)$$

The Hamiltonian H is rather complicated, non-diagonal and split up according to

$$H = H_M + H_V + H_S + H_F. \quad (2.7)$$

Its *mass part* H_M ,

$$H_M = \sum_n \frac{1}{n} [a_n^\dagger a_n (m_B^2 + g^2 \alpha_n) + b_n^\dagger b_n (m_F^2 + g^2 \beta_n) + d_n^\dagger d_n (m_F^2 + g^2 \gamma_n)], \quad (2.8)$$

depends on the bare Fermion and Boson masses, and on the self-induced inertias α, β and γ , defined below. The *vertex part* H_V of the Hamiltonian is linear in the coupling constant $g \equiv \frac{\lambda}{\sqrt{4\pi}}$,

$$\begin{aligned} H_V = gm_F \sum_{k,l,m} & (b_k^\dagger b_m c_l^\dagger + b_m^\dagger b_k c_l) [\{k+l-m\} + \{k+l-m\}] \\ & (d_k^\dagger d_m c_l^\dagger + d_m^\dagger d_k c_l) [\{k+l-m\} + \{k+l-m\}] \\ & (b_k d_m c_l^\dagger + d_m^\dagger b_k c_l) [\{k-l+m\} + \{k-l+m\}], \end{aligned} \quad (2.9)$$

while the *seagull part*

$$\begin{aligned} H_S = g^2 \sum_{k,l,m,n} & b_k^\dagger b_m c_l^\dagger c_n [\{k-n|l-m\} + \{k+l-m-n\}] \\ & + d_k^\dagger d_m c_l^\dagger c_n [\{k-n|l-m\} + \{k+l-m-n\}] \\ & + (d_k b_m c_l^\dagger c_n^\dagger + b_m^\dagger d_k c_n c_l) \{l-k|n-m\}, \end{aligned} \quad (2.10)$$

and the *fork part* H_F of the Hamiltonian, i.e.

$$\begin{aligned}
H_F = g^2 \sum_{k,l,m,n} & (b_k^\dagger b_m c_l^\dagger c_n^\dagger + b_m^\dagger b_k c_n c_l) \{k+l|n-m\} \\
& + (d_k^\dagger d_m c_l^\dagger c_n^\dagger + d_m^\dagger d_k c_n c_l) \{k+l|n-m\} \\
& + b_k^\dagger d_m^\dagger c_l^\dagger c_n \{ \{k-n|m+l\} + \{k+l|m-n\} \} \\
& + d_m b_k c_n^\dagger c_l \{ \{k-n|m+l\} + \{k+l|m-n\} \},
\end{aligned} \tag{2.11}$$

are proportional to g^2 . We use the abbreviation $c_n \equiv \frac{a_n}{\sqrt{n}}$. The matrix element $\{n|m\}$ conserves the light cone momentum and has the values

$$\{n|m\} = \begin{cases} 0 & \text{if } n = 0 \text{ and } m = 0, \\ \frac{1}{n} \delta_{m,-n} & \text{if } n \neq 0 \text{ and } m \neq 0. \end{cases} \tag{2.12}$$

The self-induced inertias depend explicitly on the momentum cutoff Λ , i.e.

$$\begin{aligned}
\alpha_n &= \sum_{m=1}^{\Lambda} \{n-m|m-n\} - \{n+m|-m-n\}, \\
\beta_n &= \sum_{m=1}^{\Lambda} \frac{n}{m} \{n-m|m-n\} \quad \text{and} \quad \gamma_n = \sum_{m=1}^{\Lambda} \frac{n}{m} \{n+m|-m-n\},
\end{aligned} \tag{2.13}$$

and will be discussed to some detail in the next section.

As for the notation, we shall label the eigenvalues of H or of KH

$$M^2 |i\rangle = M_i^2 |i\rangle, \tag{2.14}$$

as opposed to the diagonal element for each the Fock state $|i\rangle$, i.e.

$$D_i = \langle i| M^2 |i\rangle = D_i = \langle i| H |i\rangle K. \tag{2.15}$$

Since K is diagonal, H and M^2 have the same eigenstates. After renormalization, M^2 has only positive eigenvalues. In line with conventional interpretation, one

identifies the lowest eigenstate of M^2 with the physical particle of charge Q . The physical boson has charge $Q = 0$ and physical mass \tilde{m}_B , the physical fermion has charge $Q = 1$ and a fixed mass \tilde{m}_F . This can be achieved by the freedom to choose the mass parameters m_B and m_F , the bare masses as they appear in the Lagrangian. The *renormalization* of the masses, i.e. the finding of the functions

$$m_B = m_B(\tilde{m}_F, \tilde{m}_B, g, K, \Lambda) \quad \text{and} \quad m_F = m_F(\tilde{m}_F, \tilde{m}_B, g, K, \Lambda) \quad (2.16)$$

is the major problem one faces in the numerical work for strong coupling. In principle, one should renormalize also the coupling constant, but this finite renormalization can be postponed until dealing with a scattering theory.

The structure of the solutions depend to some extent on the choices of the physical masses. Although we have done calculations with various parameters, we shall present results for only two sets. The first one may be taken as a representative for $\tilde{m}_B \ll \tilde{m}_F$, i.e.

$$\tilde{m}_F = 6.7 \quad \text{and} \quad \tilde{m}_B = 1.0 \quad (2.17)$$

in units of the pion mass, for example, and was used by Serot^[3] in order to produce reasonable binding in one-dimensional nuclei. The second one, i.e.

$$\tilde{m}_F = 0.3 \quad \text{and} \quad \tilde{m}_B = 1.0, \quad (2.18)$$

is introduced mostly for the purpose of comparison with the results of Brooks and Frautschi^[1] and may be taken as a representative for $\tilde{m}_B \gg \tilde{m}_F$.

3. The Self-induced Inertias and the Fock Space.

The self-induced, instantaneous inertias arise from normal ordering the sea gull graphs^[2]. This murky birth might be an explanation why they have apparently not been noticed before. Their existence is not specific to a scalar theory nor to one space dimension; they will appear also in the three dimensional treatment of QED and QCD. As a matter of fact, they play an important role in the renormalization of the bare masses and in finding the exact spectrum. If one analyses their origin in time-ordered perturbation theory in the way done by Weinberg^[4], they turn out closely related to vacuum polarization and self-energy terms. In a way, they represent a resummation of certain graphs to all orders.

It is therefore instructive to analyse their dependence on the momentum cut-off in somewhat greater detail. With the identity

$$\frac{n}{m(n-m)} = \frac{1}{m} - \frac{1}{m-n}, \quad (3.1)$$

the self-induced inertias, as defined in Eqs. (2.13), become for the fermions for example

$$\beta_n = -\frac{1}{n} + \sum_{m=1}^{\Lambda} \frac{1}{m} - \sum_{m=1, m \neq n}^{\Lambda} \frac{1}{m-n}. \quad (3.2)$$

Since $\frac{1}{m-n}$ changes sign in the sum, one rewrites this as

$$\sum_{m=1, m \neq n}^{\Lambda} \frac{1}{m-n} = \sum_{m=1}^{n-1} \frac{1}{m-n} + \sum_{m=n+1}^{2n-1} \frac{1}{m-n} + \sum_{m=2n}^{\Lambda} \frac{1}{m-n},$$

and notes that the two first terms cancel each other. Treating α_n and γ_n in the

same way one gets

$$\begin{aligned}
\alpha_n &= -\frac{1}{n} - \sum_{m=1}^{\Lambda} \frac{1}{m+n} - \sum_{m=2n+1}^{\Lambda} \frac{1}{m-n}, \\
\beta_n &= -\frac{2}{n} + \sum_{m=1}^{\Lambda} \frac{1}{m} - \sum_{m=2n+1}^{\Lambda} \frac{1}{m-n}, \quad \text{and} \\
\gamma_n &= + \sum_{m=1}^{\Lambda} \frac{1}{m} - \sum_{m=1}^{\Lambda} \frac{1}{m+n}.
\end{aligned} \tag{3.3}$$

One notes already at this point that logarithmic divergences pile up for α_n , while they cancel in β_n and γ_n . To be more specific, one replaces summation by integration, i.e. substitutes $\sum_{m=i}^{\Lambda}$ by $\int_{i-\frac{1}{2}}^{\Lambda+\frac{1}{2}} dm$ to obtain in lowest order of $\frac{n}{\Lambda+\frac{1}{2}}$

$$\begin{aligned}
\alpha_n &\sim 2 \ln(2n+1) - \frac{1}{n} - 2 \ln(2\Lambda+1), \\
\beta_n &\sim \ln(2n+1) - \frac{2}{n} + \frac{n}{\Lambda+\frac{1}{2}}, \quad \text{and} \\
\gamma_n &\sim \ln(2n+1) - \frac{n}{\Lambda+\frac{1}{2}}.
\end{aligned} \tag{3.4}$$

Obviously, the boson inertias diverge like $\ln \Lambda$ plus negligible terms in $(\frac{1}{\Lambda})^2$, while the divergence cancels in the fermionic inertias with terms in $\frac{1}{\Lambda}$ surviving. Note that both the differences $\alpha_n - \alpha_m$ and the fermionic inertias β and γ become independent of Λ in the limit $\Lambda \rightarrow \infty$.

The approximation (3.4) reproduces the exact numerical values, as given in Tables 1 - 3 within a few percent. The numbers show quite nicely the expected convergence with increasing cut-off, but the convergence is slow. In the numerical work, we use the value $\Lambda = 2048$, if not noted otherwise. As we have tested in various calculations, this value is sufficiently large to erase the dependence on Λ

to within 3 significant digits in all numbers quoted below, *in particular in the mass spectra.*

In order to solve the spectra, one chooses the Fock space representation, and enumerates all possible Fock states with the same eigenvalues of the momentum K and the charge Q . As discussed elsewhere^[2], their number is finite, and we refer to it in short as the Fock space dimension. A typical Fock state can be written as

$$\begin{aligned}
 |i\rangle &= |n_1, n_2, \dots, n_N; \bar{n}_1, \bar{n}_2, \dots, \bar{n}_N; \tilde{n}_1^{\tilde{m}_1}, \tilde{n}_2^{\tilde{m}_2}, \dots, \tilde{n}_N^{\tilde{m}_N}\rangle \\
 &\equiv (b_{n_1} b_{n_2} \dots b_{n_N})^\dagger (d_{\bar{n}_1} d_{\bar{n}_2} \dots d_{\bar{n}_N})^\dagger \left(a_{\tilde{n}_1}^{\tilde{m}_1} a_{\tilde{n}_2}^{\tilde{m}_2} \dots a_{\tilde{n}_N}^{\tilde{m}_N} \right)^\dagger |0\rangle C_i.
 \end{aligned}
 \tag{3.5}$$

It is antisymmetric in the fermionic, and symmetric in the bosonic coordinates, i.e. in the N occupied momentum states n_i , which by convention carry a bar for the antifermion and a tilde for the boson momenta. The constant C_i ensures the normalization $\langle i|i\rangle = 1$ on the interval $(-L, +L)$. The finding of all Fock states with the same K and Q is a non-trivial combinatorial problem, which can be solved efficiently on a computer. As can be seen from Table 4, the Fock space dimension increases rapidly with increasing K for Q fixed, but decreases with increasing charge Q for a fixed K .

The Fock space vacuum $|0; \bar{0}; \tilde{0}\rangle = |0\rangle$ has no occupied light cone momentum states at all. It has charge $Q = 0$, momentum $K = 0$, and because of the latter also an invariant mass $M = 0$. It is the only state with these quantum numbers, and therefore is an eigenstate to the Hamiltonian H : As is well known^[5], in light cone quantization the Fock space vacuum is identical with the physical vacuum, as opposed to space-time quantization.

But so far it has not been noted that other Fock states are eigenstates of the Hamiltonian as well. In fact, we can differentiate at least two classes of them.

The first class has Fock space dimension 1, similar to the vacuum state, which we refer to as *primitive states*. As one sees from Table 4, every charge sector has

at least one primitive state, the one with total momentum $K = Q(Q + 1)/2$. This is understood easily. Imagine a Fock state with no bosons and antifermions, but with N_f fermions, occupying the lowest possible momentum states, i.e. $|1, 2, \dots, N_f; \bar{0}; \tilde{0}\rangle$. The state has a total charge $Q = N_f$ and a total momentum $K = N_f(N_f + 1)/2$. It is impossible to construct any other state with the same charge and the same momentum: The Fock space dimension is 1, and the Fock state is thus an eigenstate of H .

To the second class of states we shall refer to as *angel states*: By definition they have no finite off-diagonal elements with any state. They have the structure $|0; \bar{0}; \tilde{1}^K\rangle$. As they do not interact, they are pure, like angels. Angels contain neither fermions nor antifermions, and therefore have charge $Q = 0$. As a condensate of momentum 1 bosons they have total momentum K . Let us study, how the Hamiltonian acts on these states. All terms with destruction operators b_n and d_m vanish, because the condensate is a vacuum with respect to fermions or antifermions. The only non-vanishing contributions of H_V must have the operator structure $d_k^\dagger b_l^\dagger a_1$, but the corresponding matrix element $\{k + l | -1\}$ vanishes for any positive k or l . A similar result holds for H_S . The only non-vanishing terms must have the structure $d_k^\dagger b_l^\dagger a_1 a_1$, but the corresponding matrix element $\{k - 1 | 1 - l\}$ vanishes for $k = l = 1$. Thus, angels are eigenstates of H with an invariant mass squared

$$M_A^2 = K^2(m_B^2 + g^2 \alpha_1). \quad (3.6)$$

4. The Mass Spectrum as Function of Harmonic Resolution.

The Fock space dimension not only is finite, it can be as small as 1. Since a 2 by 2 matrix can be trivially diagonalized, a number of cases can be treated analytically. In the sequel, we shall increase the resolution stepwise in order to see how the invariant mass spectrum gains complexity as a function of the harmonic resolution K .

4.1 HARMONIC RESOLUTION $K = 1$.

According to Table 4, one has only primitive states for $K = 1$. Their Fock representation and diagonal elements D are explicitly

$$\begin{aligned} |b\rangle &= |0; \bar{0}; \tilde{1}^1\rangle \quad \text{with} \quad D_b = m_B^2 + \alpha_1 g^2, \quad \text{and} \\ |f\rangle &= |1; \bar{0}; \tilde{0}\rangle \quad \text{with} \quad D_f = m_F^2 + \beta_1 g^2. \end{aligned} \quad (4.1)$$

It is natural to identify the single Fock state in the charge 0 sector with the physical boson state $|b\rangle$, and the single Fock state in the charge 1 sector with the physical fermion $|f\rangle$. Renormalization is easy in this case, i.e.

$$m_F^2 = \tilde{m}_F^2 - \beta_1 g^2 \quad \text{and} \quad m_B^2 = \tilde{m}_B^2 - \alpha_1 g^2. \quad (4.2)$$

The mass spectrum is reduced to the identity, $M_f = \tilde{m}_F$ and $M_b = \tilde{m}_B$. At the lowest level of resolution, one has thus a tautology.

4.2 HARMONIC RESOLUTION $K = 2$.

Increasing the resolution by one unit, one has already three Fock states for $Q = 0$, i.e.

$$\begin{aligned} |1\rangle &= |0; \bar{0}; \tilde{2}^1\rangle \quad \text{with} \quad D_1 = m_B^2 + g^2 \alpha_2, \\ |2\rangle &= |1; \bar{1}; \tilde{0}\rangle \quad \text{with} \quad D_2 = 4m_F^2 + 2g^2(\beta_1 + \gamma_1), \\ |3\rangle &= |0; \bar{0}; \tilde{1}^2\rangle \quad \text{with} \quad D_3 = 4m_B^2 + 4g^2 \alpha_1. \end{aligned} \quad (4.3)$$

All off-diagonal elements vanish: The Fock state $|3\rangle$ is an angel state, which cannot interact with any other state. The interaction $\langle 1|H|2\rangle$ is zero, because

the vertex part has a vanishing matrix element for equal fermion and antifermion momenta. Thus, all three Fock states in the charge 0 sector are exact eigenstates of the Hamiltonian, with invariant masses $M_i^2 = D_i$, provided one has renormalized the bare masses.

Boson and Angel Renormalization. How does one have to interpret the states, Eq. (4.3)? One of them must be taken as the fermion-antifermion, the quasi-pion state; i.e. $|f\bar{f}\rangle = |2\rangle$. But which one of the two remaining states is the better boson state $|b\rangle$? One cannot label the states according to the boson number $a_n^\dagger a_n$, since it does not commute with the Hamiltonian. For small coupling constant, D_1 is less than D_3 , and therefore one has to identify $|b\rangle = |1\rangle$ in line with convention. This choice fixes the bare mass in *boson renormalization*

$$m_B^2 = \tilde{m}_B^2 - g^2 \alpha_2. \quad (4.4)$$

By substitution, one obtains the invariant mass of the angel state $|bb\rangle$

$$M_{bb}^2 = 4\tilde{m}_B^2 - 4g^2(\alpha_2 - \alpha_1). \quad (4.5)$$

According to Table 1, $\alpha_2 - \alpha_1$ is positive; eventually, beyond the critical value of the coupling constant

$$g_c(K=2) = \tilde{m}_B \sqrt{\frac{3}{4(\alpha_2 - \alpha_1)}}, \quad (4.6)$$

the angel mass will intersect the boson mass. For even larger values, one is in conflict with convention, since the lowest eigenvalue is not \tilde{m}_B . One maintains the conventional interpretation by switching over to *angel renormalization*

$$m_B^2 = \frac{1}{4}\tilde{m}_B^2 - g^2 \alpha_1 \quad \text{for } g \geq g_c(2). \quad (4.7)$$

For arbitrary K the angel renormalization is given by

$$m_B^2 = \left(\frac{\tilde{m}_B}{K}\right)^2 - g^2 \alpha_1 \quad \text{for } g \geq g_c(K), \quad (4.8)$$

according to Eq. (3.6). Now, the angel becomes the physical boson with invariant

mass $M_{bb} = \tilde{m}_B$, while the “boson” becomes an excited state with invariant mass

$$M_b = \sqrt{\left(\frac{\tilde{m}_B}{2}\right)^2 + g^2(\alpha_2 - \alpha_1)} \quad \text{for } g \geq g_c(2). \quad (4.9)$$

Its mass is *always* larger than $\frac{\tilde{m}_B}{2}$.

Fermion Renormalization. The invariant mass of the quasi-pion state can be given only when the bare mass m_F is expressed in terms of the physical masses, which shall be done next. According to Table 4, one can construct 2 Fock states for charge $Q = 1$, i.e.

$$\begin{aligned} |1\rangle &= |2; \bar{0}; \tilde{0}\rangle \quad \text{with } D_1 = m_F^2 + g^2\beta_2, \\ |2\rangle &= |1; \bar{0}; \tilde{1}^1\rangle \quad \text{with } D_2 = 2m_F^2 + 2m_B^2 + 2g^2(\beta_1 + \alpha_1) + g^2. \end{aligned} \quad (4.10)$$

Note that the seagull part gives the contribution g^2 in D_2 , while the vertex part of the Hamiltonian generates the interaction $\langle 1|H|2\rangle = 3m_Fg$. Of the two eigenvalues, M_1^2 and M_2^2 , the lower one is to be identified with the physical fermion mass, i.e.

$$\tilde{m}_F^2 = \frac{D_1 + D_2}{2} - \sqrt{\left(\frac{D_1 - D_2}{2}\right)^2 + (3m_Fg)^2}, \quad (4.11)$$

while the second eigenvalue shall be identified with an excited fermion $|fb\rangle$ with invariant mass M_{fb} , i.e.

$$M_{fb}^2 = \frac{D_1 + D_2}{2} + \sqrt{\left(\frac{D_1 - D_2}{2}\right)^2 + (3m_Fg)^2}. \quad (4.12)$$

Eq. (4.11) must be inverted. It is a second order equation in m_F^2 , which one can write rather transparently $(m_F^2 - A)(2m_F^2 - B) - 9m_F^2g^2 = 0$, where A and B are related to the diagonal elements by $A = m_F^2 + \tilde{m}_F^2 - D_1$ and $B = 2m_F^2 + \tilde{m}_F^2 - D_2$

or explicitly

$$A = \tilde{m}_F^2 - g^2 \beta_2 \quad \text{and} \quad B = \tilde{m}_F^2 - 2m_B^2 - 2g^2(\beta_1 + \alpha_1) - g^2. \quad (4.13)$$

The solution is

$$m_F^2 = \frac{1}{4} \left[2A + B + 9g^2 + \sqrt{(2A - B)^2 + 18g^2(2A + B) + (9g^2)^2} \right]. \quad (4.14)$$

The sign in front of the square root has been chosen in order to get the right value for vanishing off-diagonal matrix element, i.e. $m_F^2 = A$. One should note that m_F depends on m_B only through B .

The Mass Spectrum. Having constructed explicitly the two functions $m_B(\tilde{m}_F, \tilde{m}_B, g, K = 2, \Lambda)$ and $m_F(\tilde{m}_F, \tilde{m}_B, g, K = 2, \Lambda)$, one can calculate the spectrum. In *boson renormalization*, i.e. for $g \leq g_c$, the expression

$$B = \tilde{m}_F^2 - 2\tilde{m}_B^2 + 2g^2(\alpha_2 - \alpha_1 - \beta_1) - g^2 \quad (4.15)$$

has to be inserted into the expression for m_F , Eq. (4.14), which yields the *three physical boson masses*

$$M_b = \tilde{m}_B, \quad M_{bb} = \frac{\tilde{m}_B}{2} \sqrt{1 - \frac{3}{4} \left(\frac{g}{g_\mu} \right)^2}, \quad \text{and} \quad M_{f\bar{f}} = 2m_F, \quad (4.16)$$

as well as the *two physical fermion masses* $M_f = \tilde{m}_F$ and M_{f_b} . Use was made of $\beta_1 + \gamma_1 = 0$, which holds for large Λ to very high precision (see Tables). The explicit expression for $M_{f\bar{f}}$ in terms of \tilde{m}_F and \tilde{m}_B is rather complicated. Similarly, in *angel renormalization*, one has to use

$$B = \tilde{m}_F^2 - \frac{1}{2}\tilde{m}_B^2 - 2g^2\beta_1 - g^2, \quad (4.17)$$

in order to obtain the physical boson masses

$$M_b = \frac{\tilde{m}_B}{2} \sqrt{1 + 3 \left(\frac{g}{g_c} \right)^2}, \quad M_{bb} = \tilde{m}_B, \quad \text{and} \quad M_{f\bar{f}} = 2m_F. \quad (4.18)$$

The physical fermion masses have the same form as above.

Independence of Cut-off Λ . One should note that the physical masses do not depend on Λ in the limit $\Lambda \rightarrow \infty$. The self-induced boson inertias appear in the combination $\alpha_2 - \alpha_1$. Differences in α_n , as well as the fermion inertias β_n and γ_n , are independent of Λ in this limit, as discussed above in section 3.

4.3 HARMONIC RESOLUTION $K > 2$.

The Fock space dimension in the charge 0 and the charge 1 sector increases rapidly with harmonic resolution. But as can be seen from Table 4, it is still sufficiently small for $K = 3$ and $K = 4$ that we can write down the explicit matrices, as is done in Appendix B. But they are too large for the analytic evaluation of the eigenvalues or explicit renormalization in closed form. In order to be flexible, we have developed a computer code for the general case, which is described in Appendix A.

Without going any further into the details, we shall discuss now some selected numerical results, mostly with the purpose of demonstrating how the harmonic resolution K acts like a measure of complexity.

Selecting the three values $K = 2, 4$ and 6, we present in Fig. 1 the invariant mass spectra of the charge 0 sector, as obtained for the parameter set Eq. (2.17), i.e. for $\tilde{m}_B \ll \tilde{m}_F$. Because of the latter, the spectrum separates into two clusters of states. The lower one appears around the boson mass \tilde{m}_B , the higher one around the quasi-pion mass of $M_{f\bar{f}} \sim 2\tilde{m}_F$, since fermions and antifermions must come in pairs. These numbers are calculated with the renormalized masses, of course, and to be complete we present them in Figs. 2 and 3. We have made sure by large scale variations, that we are in a regime of the ultraviolet-cut-off (i.e. $\Lambda = 2048$), where the numbers do not depend on Λ within three significant figures.

The lowest invariant mass, the boson mass \tilde{m}_B appears first for $K = 1$, and repeats itself in any subsequent value of the harmonic resolution. This, of course, occurs by construction, but one should note that the corresponding eigenstates

gain considerable structure in terms of Fock space components, in particular when the coupling constant becomes large. The repetition of these states with K are *manifestations of the same physical particle, viewed however with increasing resolution.*

The same mechanism is observed for the ‘excited’ physical bosons, for example for the first excited state. For $K = 2$ it is the angel state, as defined and discussed above. The same eigenvalue can be observed for $K = 4$ and $K = 6$, albeit with a different eigenfunction (the angel state proper turns out to have always the largest mass within the lower cluster). The aspect of repetition includes even the bunching of the states around the critical coupling constant g_c , as defined by Eq. (4.6).

The repetition of states occurs not only for the boson cluster, but appears also for the upper, the quasi-pion cluster. *Every state* which appears for $K = 2$ appears also for $K = 3$ (not shown) and for $K = 4$ with almost the same invariant mass as manifestation of the *same physical particle*; every state of $K = 4$ reappears for $K = 5$ and $K = 6$, and so on. On the other hand, every *physical particle* has a threshold value of K , for which it appears first, a property which is amazingly similar to the charge, as seen from Table 4.

5. Comparison with Space-Time Quantization.

The rather extensive discussion of the spectra as function of increasing harmonic resolution K allows also for the following conclusion: As long as one is interested only in the invariant mass of a certain physical particle, as function of the coupling constant, one can restrict to the case of its first appearance. Thus, the most important aspects of the quasi-pion $|f\bar{f}\rangle$ are given already by the analytically soluable case of $K = 2$, see section 4.2. Its invariant mass as function of the coupling constant is plotted in Fig. 4 once for the the cut-off $\Lambda = 2048$ and once for $\Lambda = 8$. They were calculated from the analytical expressions as given in

section 4.2 for the parameter set Eq.(2.18) and are an example for $\tilde{m}_B/\tilde{m}_F \gg 1$. The plot gives also all other physical states, in the above notation.

The difference in the two quasi-pion curves $M_{f\bar{f}}$ is striking, in particular for coupling constants $1.3 \leq \lambda \leq 1.7$. For $\Lambda = 8$ no quasi-pion state is possible in this region. The analysis on the solutions of Eq.(4.14) is somewhat lengthy. Suffice it to say that depending on the ratio \tilde{m}_B/\tilde{m}_F the absence of $M_{f\bar{f}}$ is caused by a delicate cancelation in Eq.(4.14), such that m_F^2 may even become negative. This is reflected also in Fig.5, where the renormalized fermion and boson masses are plotted versus the coupling constant. This cancellation has almost no effect on the other physical masses; they are quantitatively but not qualitatively different for the two values of Λ . (M_{fb} has actually been calculated with the negative value of m_F^2 for $\Lambda = 8$.) For large Λ such difficulties do not occur.

The parameter set $\tilde{m}_F/\tilde{m}_B = 0.3$ was chosen with the purpose of comparing the above results to the recent work of Brooks and Frautschi^[1] in space-time quantization. Their final result for the invariant mass spectrum looks more like the right than like the left part of Fig. 4. In particular, their quasi-pion intersects the vacuum state above a certain value of the coupling constant, λ_x , but their value is about twice as large as ours. Brooks and Frautschi express concern about this intersection. They mention an increase of λ_x with increasing cut-off in the (space-time) momentum, and surmise, that λ_x tends to infinity for large cut-off. Also in the light cone results, the intersection λ_x tends to larger values, for example increasing the cut-off from $\Lambda = 8$ to $\Lambda = 10$. But this ceases to be true for larger cut-offs. At $\Lambda \sim 27$ already, no intersection occurs at all, at any value of the coupling constant. For even larger values of Λ , the quasi-pion mass approaches gradually the asymptotic value plotted in the left part of the figure. In space-time quantization, one has to introduce an additional cut-off in the boson number. This, and the lack of information on the momentum cut-off, or at least on the dimensions of the matrices actually diagonalized, makes a more quantitative comparison rather difficult. We conclude in view of the qualitative agreement with the $\Lambda = 8$ case that the cut-offs in space-time quantization have

been taken too small, despite the fact, that the matrix dimensions were most likely at the edge of numerical feasibility.

The too-small cut-offs can explain also why the sharp kink of the boson-angel system at $\lambda_c = \sqrt{\frac{3\pi}{\alpha_2 - \alpha_1}} = 2.4715$ is not observed in space-time quantization. This kink represents a crossing of states; at $\lambda = \lambda_c$ the two states are degenerate. In practice, it is difficult to reproduce degeneracies like this one in another representation, in particular if the space is not large enough. In general, the sharp structures are washed out; instead of a crossing one will observe smoothly repelling curves. Brooks and Frautschi observe a *non-unique mass renormalization*. The numerical value of the branch point ($\lambda \sim 2.4$, as read off from their figure), agrees well with our λ_c . Although perhaps accidental, this gives a hint for the conclusion that their observation is a remainder of the underlying structure, the *boson and angel renormalization* as discussed in section 4.2.

6. Conclusions and Outlook

In a preceding and in the present paper we have investigated the bound state problem of fermions interacting with scalar bosons in one space and one time dimension. Using discretized light cone quantization this model is strictly solvable at almost any level of refinement. The level of refinement is governed by the value of the quantum number K . This quantity has two aspects. On the one hand, it is closely related to the total light cone momentum P^+ ; i.e. $K = LP^+/2\pi$, where L is the length of the periodic interval in the light cone distance x^- . The introduction of this dimensional parameter is necessary to denumerate the momentum states. On the other hand, K can be viewed as the integral ratio between this box size and the Compton wave length of a physical particle (state) with mass M , i.e. $K = L/\lambda_C$ with $\lambda_C = \frac{2\pi\hbar}{Mc}$. For fixed mass, the larger L , the closer one is to the continuum limit and the more complex becomes the spectrum of physical particles with mass close to M and the more complex becomes its eigenfunction in terms of free Fock states.

Both the eigenvalue of the invariant mass operator and its eigenfunctions are independent of the two formal parameters of the theory, the box size L and (at large Λ) the (light cone) momentum cut-off Λ .

Our numerical results are not in conflict with the recent numerical work in space-time quantization by Brooks and Frautschi, but it appears as if the calculated spectrum is still sensitive to the cutoff shown for the (space-time) momentum. It must be noted, that the space-time approach is less economical by orders of magnitude than the present light cone approach.

In addition to the practical advantages of discretized light cone quantization for obtaining bound state spectra and wavefunctions, there are also a number of conceptual advantages:

Unlike equal time formalism, a consistent Fock state representation exists at equal x^+ . The basis is orthonormal with positive norm components summing to unit probability.

There is a precise theory of observables in terms of light cone Fock state wavefunctions. In particular, matrix element of currents and form factors can be directly expressed as a convolution of light-cone wavefunctions in momentum space. Structure functions for inclusive reactions and distribution amplitudes for exclusive reactions also have an immediate representation in this basis^[5].

Quantization of non-abelian gauge theory at equal x^+ is reviewed in refs.(5,6). By choosing the light-cone gauge $A^+ = 0$, dependent degrees of freedom are eliminated through the equation of motion as in paper I. In this gauge there are no ghosts or negative-metric propagating vector or scalar fields.

Unlike lattice gauge theory with the standard nearest-neighbor approximation to the derivative of the fermion field, the discretized light cone quantization approach does not lead to doubling of the fermion states. This derivative is represented as the factor $1/n$ in the massive part of the hamiltonian H_M in momentum space.

Unlike path integral formulations, fermions and bosons are treated on an equal basis in the light cone hamiltonian formulation.

The ease of generating exact solutions to a simple field theoretic problem creates opportunities for further development and investigation:

It appears possible to treat higher particle systems (nuclei) with reasonable numerical effort in $1 + 1$ dimensions. In fact, the major part of the numerical work is taken up by the renormalisation of the masses, since the Hamiltonian has the largest dimensions in the charge 0 and the charge 1 sector.

The essential and surprising feature of the discretized light cone approach is the appearance of finite dimensional Hamiltonians. Usually such a property is related to a discrete group and a compact Lie algebra. We have no idea to which group the present approach is isomorphous. Its discovery could be of great help in finding the most economic approach to $3+1$ dimensions.

The ultimate goal is to obtain non-perturbative solutions in $3+1$ dimensions. If one introduces light cone variables in a preferred direction $z \pm t$ and parameterizes the perpendicular directions with variables L_z and transverse momenta k_{\perp}^2 one at least reduces the dimensionality of the problem significantly compared to space-time quantization^[7].

ACKNOWLEDGEMENTS

One of us (HCP) thanks the Max-Planck-Gesellschaft for supporting a sabbatical year and the Stanford Linear Accelerator Center and its Theory Group for their kind hospitality and the inspiring atmosphere. We also thank H. Quinn and G.P. Lepage for helpful conversations.

APPENDIX A: The numerical procedure

For minimal storage requirements in the computer, it is convenient to use an indirect addressing scheme. The Fock space information can be generated efficiently by first calculating the Boson space \mathcal{B} , i.e. all Boson states

$$|i\rangle_B = |\tilde{n}_1(\tilde{m}_1), \tilde{n}_2(\tilde{m}_2), \dots, \tilde{n}_{N_B}(\tilde{m}_{N_B})\rangle \quad , \quad i = 1, \dots, N_B,$$

which have total light cone momentum $K_B = \sum_n n a_n^\dagger a_n \leq K_{max}$, where K_{max} is equal to the value of K under consideration. In the same way one calculates the Fermi space \mathcal{F}

$$|i\rangle_F = |n_1(m_1), n_2(m_2), \dots, n_{N_F}(m_{N_F})\rangle \quad , \quad i = 1, \dots, N_F,$$

with the occupation numbers $m_i = 1$ and $K_F \leq K_{max}$. The same information can be used for calculating the Dirac space \mathcal{D} , i.e. all possible states for the diracons (= antifermions) with $K_D \leq K_{max}$. The Fock space is obtained by taking all possible combinations

$$|i\rangle = |j\rangle_F |k\rangle_D |l\rangle_B$$

for which hold

$$K = K_F + K_D + K_B \quad \text{and} \quad Q = N_F - N_D.$$

One needs to store only a mnemonic number representing all the quantum numbers of the state. If one stores for each state $|j\rangle_F$ or $|l\rangle_B$ the partial momentum (i.e. K_B), the number of occupied states (i.e. N_B), the single particle momenta n_l , and their occupation number m_l , one has to meet the Fock space storage requirements as compiled in Tables 4 and 5.

In a second step one calculates the diagonal element D_i for each Fock state. Provision was made for removing all states whose diagonal element exceeds a given cut-off D_{cut} . In this way one can cut down efficiently the large dimensions in matrix diagonalization problems, without losing too much accuracy. The method seems particularly suited for determination of the renormalized masses. In this paper, however, this option has not been used, since restriction was made to $K \leq 6$.

In a third step, the Hamiltonian matrix $K \langle j | H | i \rangle$ was calculated. The Hamiltonian has non-vanishing matrix elements only if the two states in question are *at the most, relative two-particle-two-hole states*. If these selection rules are satisfied simultaneously in the boson, the fermion and the diracon sector (which can all be done in rather fast fix point arithmetic) then the matrix element is computed (it involves one single square root operation). The set-up of the Hamiltonian matrix consumes a time negligible compared to the Fock space combinatorics, diagonalization, and renormalization.

In a fourth step, the matrix is diagonalized numerically. Standard numerical procedures are used, as provided by the Eispack package at SLAC.

Last, one must renormalize the boson and fermion masses numerically. The following procedure was chosen. (1) Take as a guess value the boson renormalization $m_B^2 = \tilde{m}_B^2 - \alpha_2 g^2$, as obtained analytically for $K = 2$. Experience shows, that this value is close to the final result, see Fig. 2. (2) With m_B fixed, search for m_F in the charge 1 sector by a combination of bisection and Newtonian *interpolation*. (3) With the so determined starting values of m_B and m_F , *iterate simultaneously* by a 4-point *interpolation* in 2 dimensions, until the lowest eigenvalues in the charge 0 and the charge 1 sector agrees within 10^{-4} with the given values \tilde{m}_B^2 and \tilde{m}_F^2 . (4) Last, if the angel mass drops below \tilde{m}_B , i.e. if $K^2(m_B^2 + \alpha_1 g^2) \leq \tilde{m}_B^2$, repeat step (2) in angel renormalization. — By large scale variation and tracing in two dimensions, it was made sure that the so obtained values are *unique*.

The routines are written in standard Fortran IV and were tested by comparing the numerical results with the analytical expressions for $K \leq 4$, as given in App. B.

APPENDIX B: The Fock Space and the Hamiltonian for $K=3$ and $K=4$

The Fock space without the angel state for $K = 3$ and $Q = 0$ has 5 components

$$\begin{aligned}
|1\rangle &= |0; \bar{0}; \tilde{3}^1\rangle & \text{with } D_1 &= m_B^2 + g^2 \alpha_3 \\
|2\rangle &= |0; \bar{0}; \tilde{1}^1, \tilde{2}^1\rangle & \text{with } D_2 &= \frac{9}{2} m_B^2 + 3g^2(\alpha_1 + \frac{\alpha_2}{2}) \\
|3\rangle &= |1; \bar{1}; \tilde{1}^1\rangle & \text{with } D_4 &= 3m_B^2 + 6m_F^2 + 3g^2(\gamma_1 + \beta_1 + \alpha_1) + \frac{3}{2} g^2 \\
|4\rangle &= |2; \bar{1}; \tilde{0}\rangle & \text{with } D_5 &= \frac{9}{2} m_F^2 + 3g^2(\gamma_1 + \frac{\beta_2}{2}) \\
|5\rangle &= |1; \bar{2}; \tilde{0}\rangle & \text{with } D_6 &= \frac{9}{2} m_F^2 + 3g^2(\frac{\gamma_2}{2} + \beta_1)
\end{aligned}$$

and correspondingly, a 5 by 5 invariant mass matrix $M^2 = HK$

	$ 1\rangle$	$ 2\rangle$	$ 3\rangle$	$ 4\rangle$	$ 5\rangle$
$\langle 1 $	D_1				
$\langle 2 $	0	D_2			
$\langle 3 $	0	0	D_3		
$\langle 4 $	$-\frac{\sqrt{3}}{2} \kappa$	$\frac{3}{\sqrt{2}} g^2$	$\frac{9}{2} \kappa$	D_4	
$\langle 5 $	$+\frac{\sqrt{3}}{2} \kappa$	$-\frac{3}{\sqrt{2}} g^2$	$\frac{9}{2} \kappa$	0	D_5

with the abbreviations $g \equiv \frac{\lambda}{\sqrt{4\pi}}$ and $\kappa = m_F g$.

The charge 1 sector for $K = 3$ has the Fock space

$$\begin{aligned}
|1\rangle &= |1; \bar{0}; \tilde{2}^1\rangle & \text{with } D_1 &= \frac{3}{2} m_B^2 + 3m_F^2 + 3g^2(\frac{\alpha_2}{2} + \beta_1) + \frac{5}{2} g^2 \\
|2\rangle &= |1; \bar{0}; \tilde{1}^2\rangle & \text{with } D_2 &= 6m_B^2 + 3m_F^2 + 3g^2(\alpha_1 + \beta_1) + 3g^2 \\
|3\rangle &= |2; \bar{0}; \tilde{1}^1\rangle & \text{with } D_3 &= 3m_B^2 + \frac{3}{2} m_F^2 + 3g^2(\alpha_1 + \frac{\beta_2}{2}) + 4g^2 \\
|4\rangle &= |3; \bar{0}; \tilde{0}\rangle & \text{with } D_4 &= m_F^2 + g^2\beta_3
\end{aligned}$$

and the invariant mass matrix M^2

	$ 1\rangle$	$ 2\rangle$	$ 3\rangle$	$ 4\rangle$
$\langle 1 $	D_1			
$\langle 2 $	0	D_2		
$\langle 3 $	$\frac{\sqrt{2}}{2} g^2$	$\frac{9}{2} \sqrt{2} \kappa$	D_3	
$\langle 4 $	$2\sqrt{2} \kappa$	$\frac{3}{2} \sqrt{2} g^2$	$\frac{5}{2} \kappa$	D_4

For $K = 4$, $Q = 0$, the Fock space without the angel state has 11 components

$$\begin{aligned}
|1\rangle &= |0; \bar{0}; \tilde{4}^1\rangle & \text{with } D_1 &= m_B^2 + g^2 \alpha_4 \\
|2\rangle &= |0; \bar{0}; \tilde{1}^1, \tilde{3}^1\rangle & \text{with } D_2 &= \frac{16}{3} m_B^2 + 4g^2(\alpha_1 + \frac{\alpha_3}{3}) \\
|3\rangle &= |0; \bar{0}; \tilde{2}^3\rangle & \text{with } D_3 &= 4(m_B^2 + g^2 \alpha_2) \\
|4\rangle &= |0; \bar{0}; \tilde{1}^2, \tilde{2}^1\rangle & \text{with } D_4 &= 10 m_B^2 + 3g^2(2\alpha_1 + \frac{\alpha_2}{2}) \\
|5\rangle &= |1; \bar{1}; \tilde{1}^2\rangle & \text{with } D_5 &= 2m_B^2 + 8m_F^2 + 4g^2(\frac{\alpha_2}{2} + \beta_1 + \gamma_1) + \frac{8}{3} g^2 \\
|6\rangle &= |1; \bar{1}; \tilde{2}^1\rangle & \text{with } D_6 &= 8m_B^2 + 4m_F^2 + 4g^2(\alpha_1 + \beta_1 + \gamma_1) + 8 g^2 \\
|7\rangle &= |2; \bar{1}; \tilde{1}^1\rangle & \text{with } D_7 &= 4m_B^2 + 6m_F^2 + 4g^2(\alpha_1 + \frac{\beta_2}{2} + \gamma_1) + \frac{44}{6} g^2 \\
|8\rangle &= |3; \bar{1}; \tilde{0}\rangle & \text{with } D_8 &= \frac{16}{3} m_F^2 + 4g^2(\frac{\beta_3}{3} + \gamma_1) \\
|9\rangle &= |1; \bar{2}; \tilde{1}^1\rangle & \text{with } D_9 &= 4m_B^2 + 6m_F^2 + 4g^2(\alpha_1 + \beta_1 + \frac{\gamma_2}{2}) + \frac{44}{6} g^2 \\
|10\rangle &= |2; \bar{2}; \tilde{0}\rangle & \text{with } D_{10} &= 4m_F^2 + 2g^2(\beta_2 + \gamma_2) \\
|11\rangle &= |1; \bar{3}; \tilde{0}\rangle & \text{with } D_{11} &= \frac{16}{3} m_F^2 + 4g^2(\beta_1 + \frac{\gamma_3}{3})
\end{aligned}$$

and the invariant mass matrix is correspondingly large, i.e.

	1)	2)	3)	4)	5)	6)	7)	8)	9)	10)	11)
$\langle 1 $	D_1										
$\langle 2 $	0	D_2									
$\langle 3 $	0	0	D_3								
$\langle 4 $	0	0	0	D_4							
$\langle 5 $	0	0	0	0	D_5						
$\langle 6 $	0	0	0	0	0	D_6					
$\langle 7 $	$-\frac{1}{3} g^2$	$-\frac{2}{\sqrt{3}} \kappa$	0	$4g^2$	$\frac{2\sqrt{2}}{3} g^2$	$6\sqrt{2} g^2$	D_7				
$\langle 8 $	$-\frac{4}{3} \kappa$	$\frac{2}{\sqrt{3}} g^2$	$2\sqrt{2} g^2$	0	$\frac{8\sqrt{2}}{3} \kappa$	$2\sqrt{2} g^2$	$\frac{10}{3} \kappa$	D_8			
$\langle 9 $	$+\frac{1}{3} g^2$	$+\frac{2}{\sqrt{3}} \kappa$	0	$-4g^2$	$\frac{2\sqrt{2}}{3} g^2$	$6\sqrt{2} \kappa$	0	0	D_9		
$\langle 10 $	0	0	0	0	0	0	6κ	0	6κ	D_{10}	
$\langle 11 $	$+\frac{4}{3} \kappa$	$-\frac{2}{\sqrt{2}} g^2$	$-2\sqrt{2} g^2$	0	$\frac{8\sqrt{2}}{3} \kappa$	$2\sqrt{2} g^2$	0	0	$\frac{10}{3} \kappa$	0	D_{11}

Finally, one gets a Fock space for $K = 4$, $Q = 1$:

$$\begin{aligned}
|1\rangle &= |1; \bar{0}; \tilde{3}^1\rangle & \text{with } D_1 &= \frac{4}{3} m_B^2 + 4m_F^2 + 4g^2(\frac{\alpha_3}{3} + \beta_1) + g^2 \\
|2\rangle &= |1; \bar{0}; \tilde{1}^1, \tilde{2}^1\rangle & \text{with } D_2 &= 6m_B^2 + 4m_F^2 + 4g^2(\alpha_1 + \frac{\alpha_2}{2} + \beta_1) + \frac{2}{3} g^2 \\
|3\rangle &= |1; \bar{0}; \tilde{1}^3\rangle & \text{with } D_3 &= 12m_B^2 + 4m_F^2 + 4g^2(3\alpha_1 + \beta_1) + 6g^2 \\
|4\rangle &= |2; \bar{0}; \tilde{2}^1\rangle & \text{with } D_4 &= 2m_B^2 + 2m_F^2 + 2g^2(\alpha_2 + \beta_2) + \frac{1}{2} g^2 \\
|5\rangle &= |2; \bar{0}; \tilde{1}^2\rangle & \text{with } D_5 &= 8m_B^2 + 2m_F^2 + g^2(2\alpha_1 + \frac{\beta_2}{2}) + \frac{32}{3} g^2 \\
|6\rangle &= |3; \bar{0}; \tilde{1}^1\rangle & \text{with } D_6 &= 4m_B^2 + \frac{4}{3} m_F^2 + 4g^2(\alpha_1 + \frac{\beta_3}{3}) + 3g^2 \\
|7\rangle &= |4; \bar{0}; \tilde{0}\rangle & \text{with } D_7 &= m_F^2 + g^2\beta_4 \\
|8\rangle &= |1, 2; \bar{1}; \tilde{0}\rangle & \text{with } D_8 &= 10m_F^2 + 4g^2(\frac{\beta_4}{4} + \frac{\beta_2}{2} + \gamma_1)
\end{aligned}$$

The invariant mass matrix M^2 is

	1\rangle	2\rangle	3\rangle	4\rangle	5\rangle	6\rangle	7\rangle	8\rangle
\langle 1	D_1							
\langle 2	0	D_2						
\langle 3	0	0	D_3					
\langle 4	$-\sqrt{\frac{3}{2}} g^2$	6κ	0	D_4				
\langle 5	0	$\frac{4}{3} g^2$	$6\sqrt{3}\kappa$	0	D_5			
\langle 6	$\frac{g^2}{\sqrt{3}}$	$\frac{8}{3}\sqrt{2}\kappa$	$2\sqrt{6}g^2$	$\frac{5}{\sqrt{2}}g^2$	$\frac{10}{3}\sqrt{2}\kappa$	D_6		
\langle 7	$+\frac{5}{\sqrt{3}}\kappa$	$\frac{5}{3}\sqrt{2}g^2$	0	$\frac{3}{\sqrt{2}}\kappa$	$\frac{4}{3}\sqrt{2}g^2$	$\frac{7}{3}\kappa$	D_7	
\langle 8	$-\frac{2}{\sqrt{3}}\kappa$	$-2\sqrt{2}g^2$	0	0	0	0	0	D_8

REFERENCES

1. E. D. Brooks and S. C. Frautschi, *Zs. Phys.* **23** (1984) 263
2. H. C. Pauli and S. J. Brodsky, SLAC-PUB-3707, to be published; in the text referred to as I
3. B. D. Serot, S. E. Koonin and J. W. Negele, *Phys. Rev.* **C28** (1983) 1679
4. S. Weinberg, *Phys. Rev.* **150** (1966) 1313
5. S. J. Brodsky, and G. P. Lepage, *Phys. Rev.* **D22** (1980) 2157
6. S. J. Brodsky, T. Huang, and G. P. Lepage, in *Banff 1981, Particle and Fields 2*, p.143-199; S. J. Brodsky, in *Short-Distance Phenomena in Nuclear Physics* (Plenum Publishing Corporation, 1983), p.141-217
7. For a related approach see W. A. Bardeen, R. B. Pearson, and E. Rabinovici, *Phys. Rev.* **21** (190) 1037

Table 1: Self-induced inertias $\tilde{\alpha}_n = \alpha_n - \alpha_1$ and $\tilde{\alpha}_1 = -\alpha_1$ as function of the cut-off Λ .

n	$\Lambda = 8$	$= 32$	$= 128$	$= 512$	$= 2048$
1	4.4218	7.1160	9.8661	12.6326	15.4023
2	1.5429	1.5029	1.5003	1.5005	1.5019
3	2.4519	2.3410	2.3340	2.3342	2.3371
4	3.1519	2.9310	2.9178	2.9180	2.9223
5	3.7750	3.3897	3.3683	3.3685	3.3743
6	4.4036	3.7670	3.7354	3.7351	3.7422
7	5.1464	4.0894	4.0457	4.0445	4.0531
8	6.3518	4.3722	4.3145	4.3112	4.3212

Table 2: Self-induced inertias β_n as function of the cut-off Λ .

n	$\Lambda = 8$	32	128	512	2048
1	-0.8750	-0.9687	-0.9922	-0.9980	-0.9995
2	0.7679	0.5635	0.5157	0.5039	0.5009
3	1.6012	1.2635	1.1903	1.1725	1.1680
4	2.2179	1.7147	1.6149	1.5911	1.5851
5	2.7679	2.0504	1.9230	1.8931	1.8855
6	3.3345	2.3207	2.1645	2.1284	2.1193
7	4.0250	2.5497	2.3631	2.3208	2.3102
8	5.1857	2.7504	2.5321	2.4835	2.4713

Table 3: Self-induced inertias γ_n as function of the cut-off Λ .

n	$\Lambda = 8$	32	128	512	2048
1	0.8889	0.9697	0.9922	0.9980	0.9995
2	1.2889	1.4403	1.4845	1.4961	1.4989
3	1.5313	1.7450	1.8102	1.8275	1.8317
4	1.6980	1.9673	2.0527	2.0755	2.0811
5	1.8211	2.1402	2.2451	2.2736	2.2806
6	1.9163	2.2806	2.4043	2.4383	2.4467
7	1.9925	2.3978	2.5398	2.5792	2.5890
8	2.0550	2.4978	2.6574	2.7022	2.7135

Table 4: The number of Fock states for given momentum K and charge Q .

Momentum K	Charge Q					
	0	1	2	3	4	5
1	1	1				
2	3	2				
3	6	4	1			
4	12	8	2			
5	21	15	5			
6	38	27	9	1		
7	63	47	18	2		
8	106	79	31	4		
9	170	130	54	8		
10	272	209	88	16	1	
11	422	329	145	29	2	
12	653	509	229	52	4	
13	986	777	362	87	7	
14	1480	1169	556	143	13	
15	2185	1739	850	228	25	1

Table 5: Storage requirements for the Fermion and Boson spaces.

Maximum Momentum K_{\max}	FERMIONS		BOSONS	
	Number of States with $K_F \leq K_{\max}$	Storage of occupied states	Number of States with $K_B \leq K_{\max}$	Storage of occupied states
1	2	10	2	10
2	3	15	4	20
3	4	20	7	37
4	11	67	12	66
5	15	93	19	111
6	19	119	30	182
7	45	341	45	287
8	58	446	67	443
9	74	576	97	667
10	92	724	139	987
11	201	1865	195	1433
12	251	2353	272	2054
13	312	2952	373	2901
14	380	3624	508	4052
15	460	4418	684	5596

FIGURE CAPTIONS

1. The mass spectrum for charge 0 versus the bare coupling constant λ .- The masses are $\tilde{m}_F = 6.7$ and $\tilde{m}_B = 1.0$, and the cut-off is $\Lambda = 2048$.- Note the increasing complexity with increasing K .
2. The bare fermion mass m_F versus the bare coupling constant λ .- The masses are $\tilde{m}_F = 6.7$ and $\tilde{m}_B = 1.0$, and the cut-off is $\Lambda = 2048$.- Note the slow convergence with increasing K .
3. The bare boson mass m_B versus the bare coupling constant λ .- The masses are $\tilde{m}_F = 6.7$ and $\tilde{m}_B = 1.0$, and the cut-off is $\Lambda = 2048$.- Note the weak dependence on K .
4. The $K = 2$ mass spectrum for charge 0 and 1 versus the bare coupling constant λ .- The masses are $\tilde{m}_F = 0.3$ and $\tilde{m}_B = 1.0$. The left part of the figure is independent of the cut-off ($\Lambda = 2048$). In the right part the cut-off is $\Lambda = 8$, far away from the Λ -independent regime; cf. also Tables 1-3.
5. The bare fermion and boson masses, m_F and m_B , respectively, versus the bare coupling constant λ .- The masses are $\tilde{m}_F = 0.3$ and $\tilde{m}_B = 1.0$. The cut-off has two values, i.e. $\Lambda = 2048$ (—) and $\Lambda = 8$ (---).- See discussion in the text.

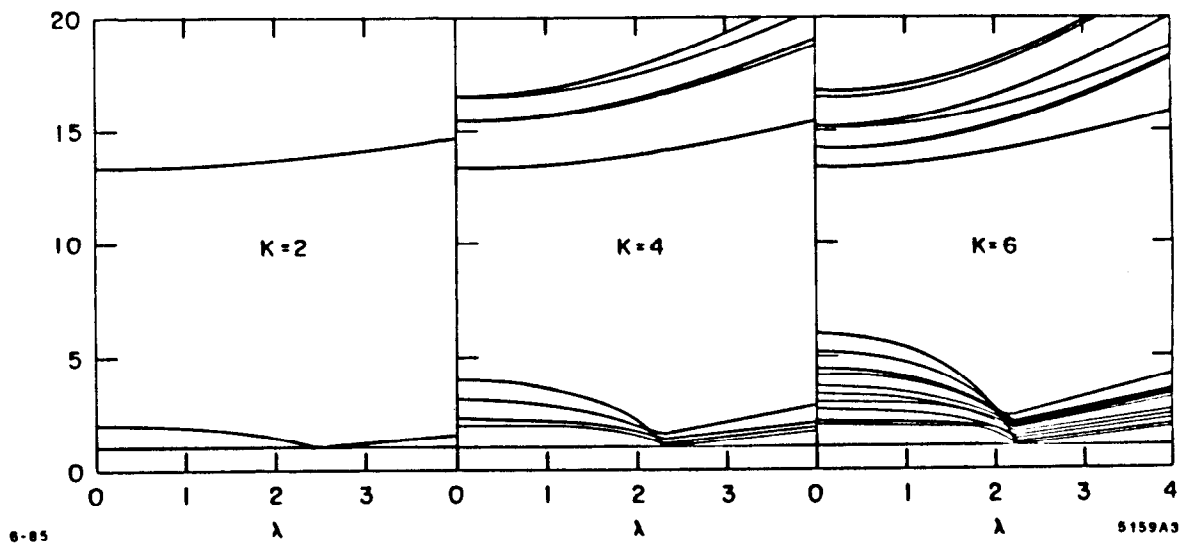


Fig. 1

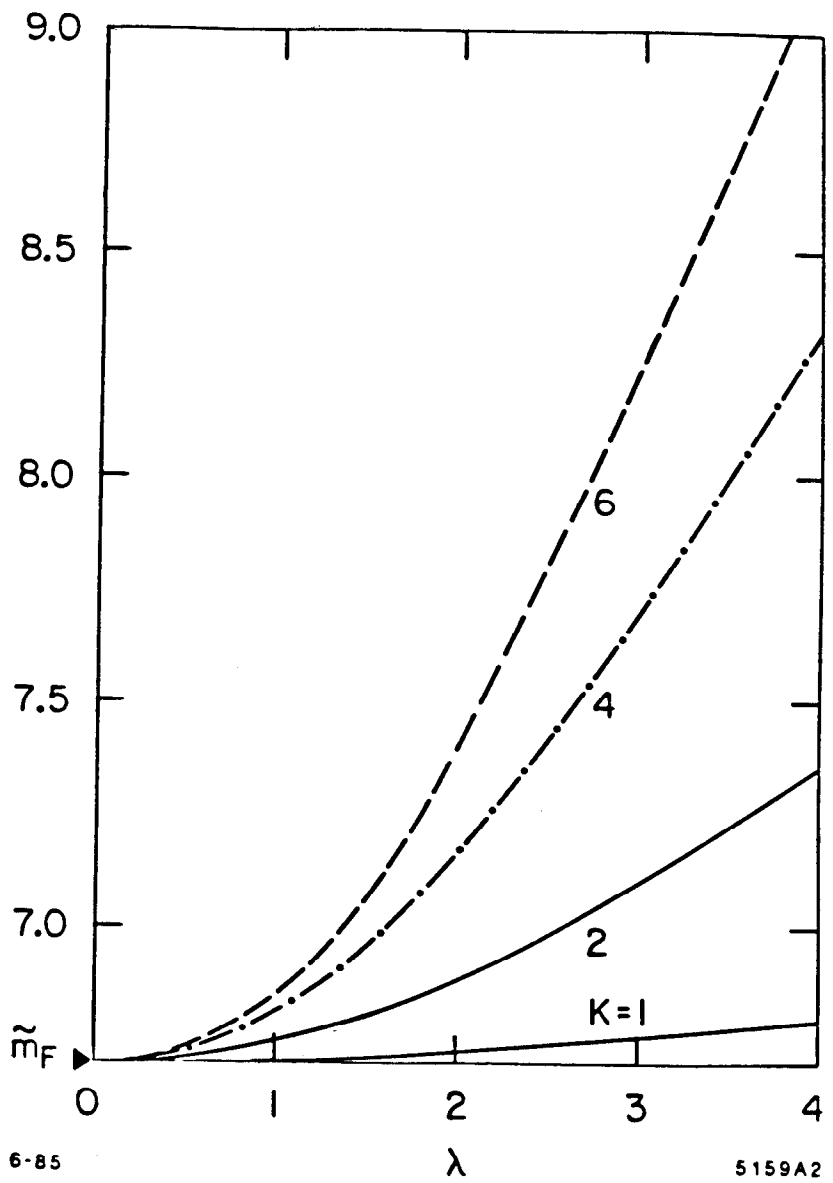


Fig. 2

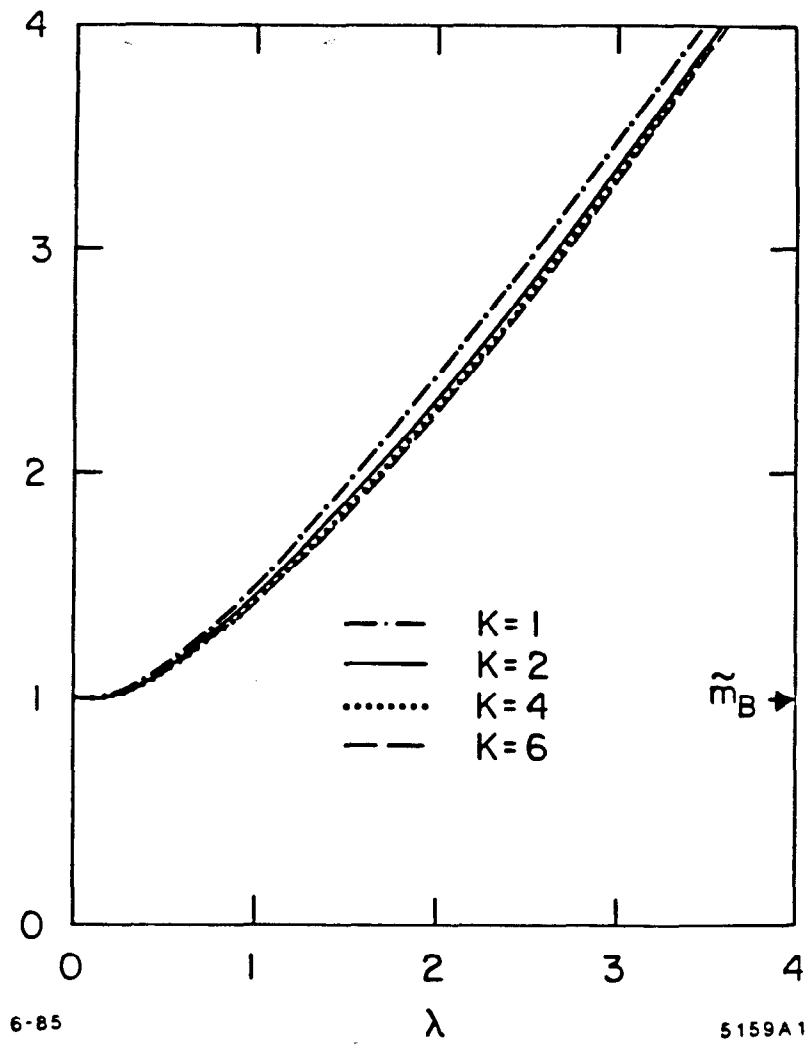


Fig. 3

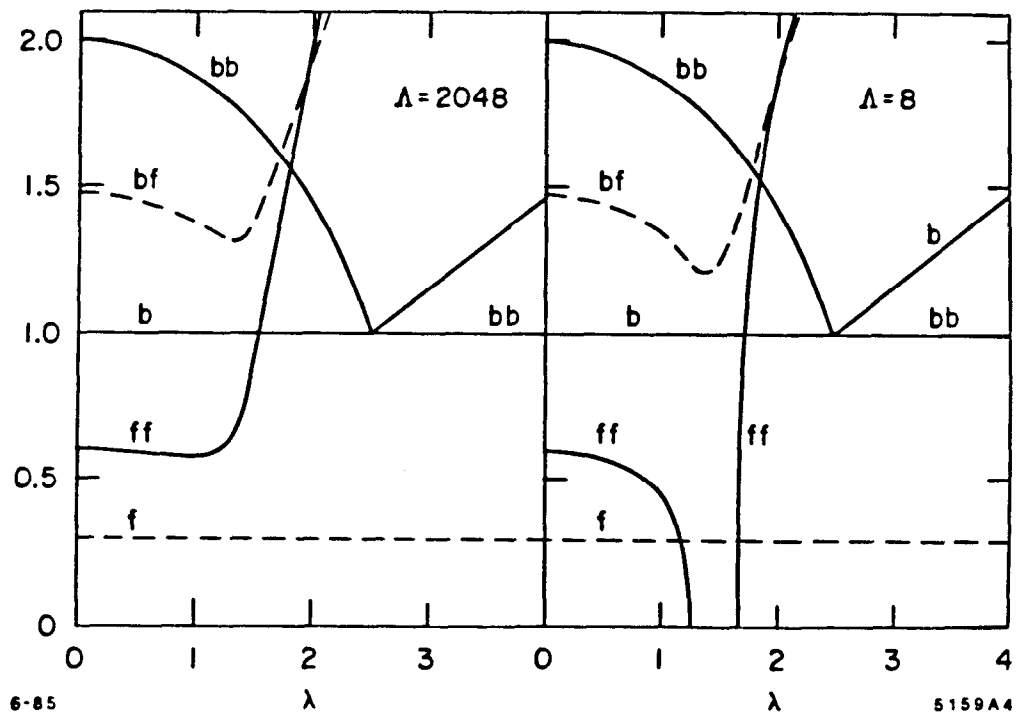


Fig. 4

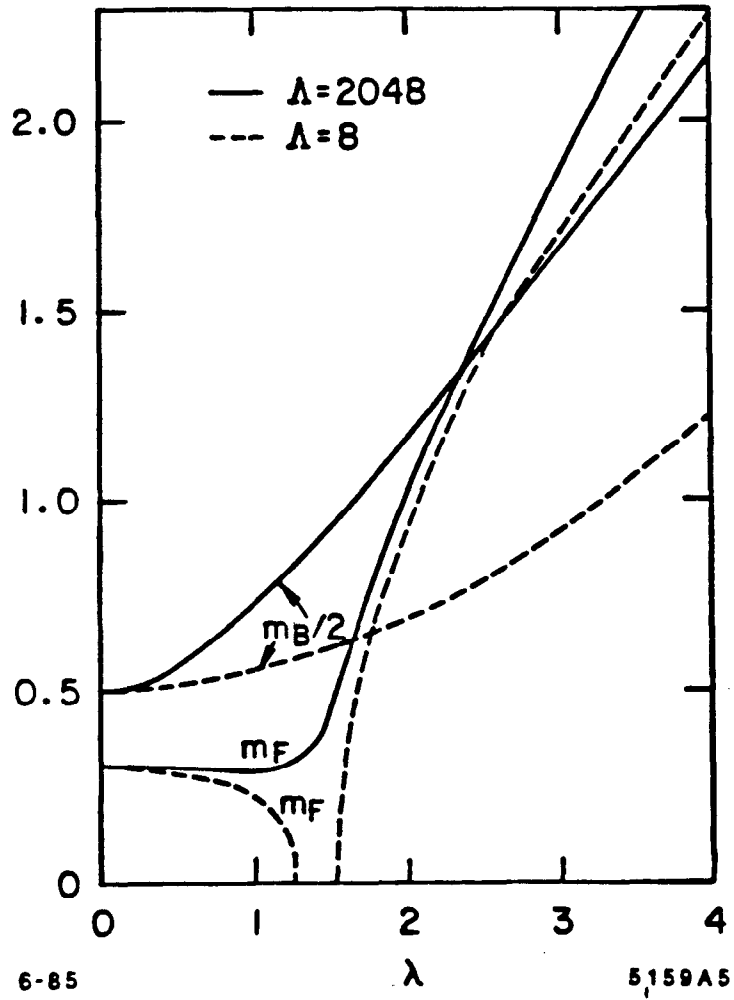


Fig. 5